

Impacts of climate change on the world's most exceptional ecoregions

Linda J. Beaumont^{a,b,1}, Andrew Pitman^c, Sarah Perkins^c, Niklaus E. Zimmermann^d, Nigel G. Yoccoz^e, and Wilfried Thuiller^b

^aDepartment of Biological Sciences, Macquarie University, Sydney, NSW 2109, Australia; ^bLaboratoire d'Ecologie Alpine, Unité Mixte de Recherche Centre National de la Recherche Scientifique 5553, Université de Grenoble, BP 53, 38041 Grenoble Cedex 9, France; ^cClimate Change Research Centre, University of New South Wales, Sydney, NSW 2052, Australia; ^dLandscape Dynamics, Swiss Federal Research Institute for Forest, Snow and Landscape Research, 8903 Birmensdorf, Switzerland; and ^eDepartment of Arctic and Marine Biology, Faculty of Biosciences, Fisheries and Economics, University of Tromsø, N-9037 Tromsø, Norway

Edited by Rodolfo Dirzo, Stanford University, Stanford, CA, and approved December 16, 2010 (received for review June 6, 2010)

The current rate of warming due to increases in greenhouse gas (GHG) emissions is very likely unprecedented over the last 10,000 y. Although the majority of countries have adopted the view that global warming must be limited to <2 °C, current GHG emission rates and nonagreement at Copenhagen in December 2009 increase the likelihood of this limit being exceeded by 2100. Extensive evidence has linked major changes in biological systems to 20th century warming. The "Global 200" comprises 238 ecoregions of exceptional biodiversity [Olson DM, Dinerstein E (2002) *Ann Mo Bot Gard* 89:199–224]. We assess the likelihood that, by 2070, these iconic ecoregions will regularly experience monthly climatic conditions that were extreme in 1961–1990. Using >600 realizations from climate model ensembles, we show that up to 86% of terrestrial and 83% of freshwater ecoregions will be exposed to average monthly temperature patterns >2 SDs (2σ) of the 1961–1990 baseline, including 82% of critically endangered ecoregions. The entire range of 89 ecoregions will experience extreme monthly temperatures with a local warming of <2 °C. Tropical and subtropical ecoregions, and mangroves, face extreme conditions earliest, some with <1 °C warming. In contrast, few ecoregions within Boreal Forests and Tundra biomes will experience such extremes this century. On average, precipitation regimes do not exceed 2σ of the baseline period, although considerable variability exists across the climate realizations. Further, the strength of the correlation between seasonal temperature and precipitation changes over numerous ecoregions. These results suggest many Global 200 ecoregions may be under substantial climatic stress by 2100.

climate impacts | climate model ensemble | conservation

Biodiversity and the maintenance of associated ecosystem goods and services are vital for human well-being, yet despite increases in conservation activity, the loss of biodiversity continues (1, 2). Although habitat degradation, fragmentation, and destruction, overexploitation, and invasive species have driven recent biodiversity loss, climate change is projected to be a major driver of extinction throughout the 21st century, both directly and via synergies with other stressors (3–6).

The rate of global climate change increased through the 20th century, and should emissions of greenhouse gases continue at or above current rates, warming in the 21st century will very likely exceed that observed over the 20th century (7). The impacts of these changes on biological systems are manifested as shifts in phenology, interactions, species distributions, morphology (8–13), and net primary productivity (14). Ultimately, the ability of species and ecosystems to respond positively to climate change will depend on species-specific characteristics (e.g., potential for rapid adaptation, phenotypic plasticity, or dispersal capability; ref. 12), current and future anthropogenic threats, the extent to which future climate regimes present conditions beyond those previously experienced, and the natural resilience of biological systems to these changes (15).

The Global 200 is a series of ecoregions selected across 30 biomes and biogeographical realms for their irreplaceability or distinctiveness, and represents an ambitious blueprint for global conservation (16). The sustainability and protection of the Global

200 would be of immense value to conservation efforts worldwide because of their richness in endemic species, high taxonomic uniqueness, unique ecological or evolutionary phenomena, global rarity, and their representation of biomes (16). However, the majority of these regions are threatened by habitat loss, fragmentation, and degradation, with 147 of 185 terrestrial and freshwater regions being classified as either vulnerable or critically endangered (CE) (16). Exposure of these ecoregions to significant climate change—in particular, extreme or novel conditions—will further undermine efforts to protect them. The identification of those ecoregions that in the future may commonly experience climate patterns that would be considered "extreme" could lead to reprioritization of conservation efforts.

Here, we assess the extent to which 132 terrestrial and 53 freshwater ecoregions of the Global 200 (Fig. 1A and Tables S1 and S2) are projected to be exposed to average monthly temperature (Tas_{μ}) and precipitation (Pr_{μ}) patterns during the 21st century, which could be considered as extreme. We define extreme as exceeding 2 SDs (σ) departing from the mean (μ) of the 1961–1990 baseline period (17), and calculate (i) deviation of 21st century monthly Tas_{μ} and Pr_{μ} from the 1961–1990 baseline, averaged over all 12 mo and (ii) the number of months for which Tas_{μ} and Pr_{μ} are projected to exceed 2σ of the baseline period.

Changes to temperature and precipitation will not have linear impacts across these ecoregions. Rather, the sensitivity of ecoregions to extreme monthly conditions will depend in part on changes to the climate variables primarily constraining productivity. For example, increases in temperature have relaxed constraints on vegetation in northern high latitudes, promoting greater net primary productivity (14, 18). In contrast, vegetation activity in ecoregions at midlatitudes and in semi-arid biomes is primarily driven by precipitation patterns (14). Increases or reductions in precipitation may release or further constrain productivity, respectively. However, as temperature across these ecoregions increases so too does the likelihood of high-autotrophic respiration induced by high temperatures, leading to greater water stress. Thus, increases in temperature may exaggerate precipitation declines, and additional stress may be placed on those ecoregions where negative correlations between temperature and precipitation strengthen. Therefore, we also assessed changes to the correlation of seasonal temperature and precipitation across each ecoregion.

To account for large variability across alternate global circulation models, we developed ensembles of climate model simulations for three emissions scenarios (B1, $n = 214$; A1B, $n = 224$; A2, $n = 173$), consisting of simulations from up to 23 climate models, with 1–76 runs per model. Realizations were weighted to

Author contributions: L.J.B., A.P., N.E.Z., N.G.Y., and W.T. designed research; L.J.B., A.P., S.P., N.E.Z., N.G.Y., and W.T. performed research; L.J.B. analyzed data; and L.J.B., A.P., S.P., N.E.Z., N.G.Y., and W.T. wrote the paper.

The authors declare no conflict of interest.

This article is a PNAS Direct Submission.

¹To whom correspondence should be addressed. E-mail: lbeaumont@rma.bio.mq.edu.au.

This article contains supporting information online at www.pnas.org/lookup/suppl/doi:10.1073/pnas.1007217108/-DCSupplemental.

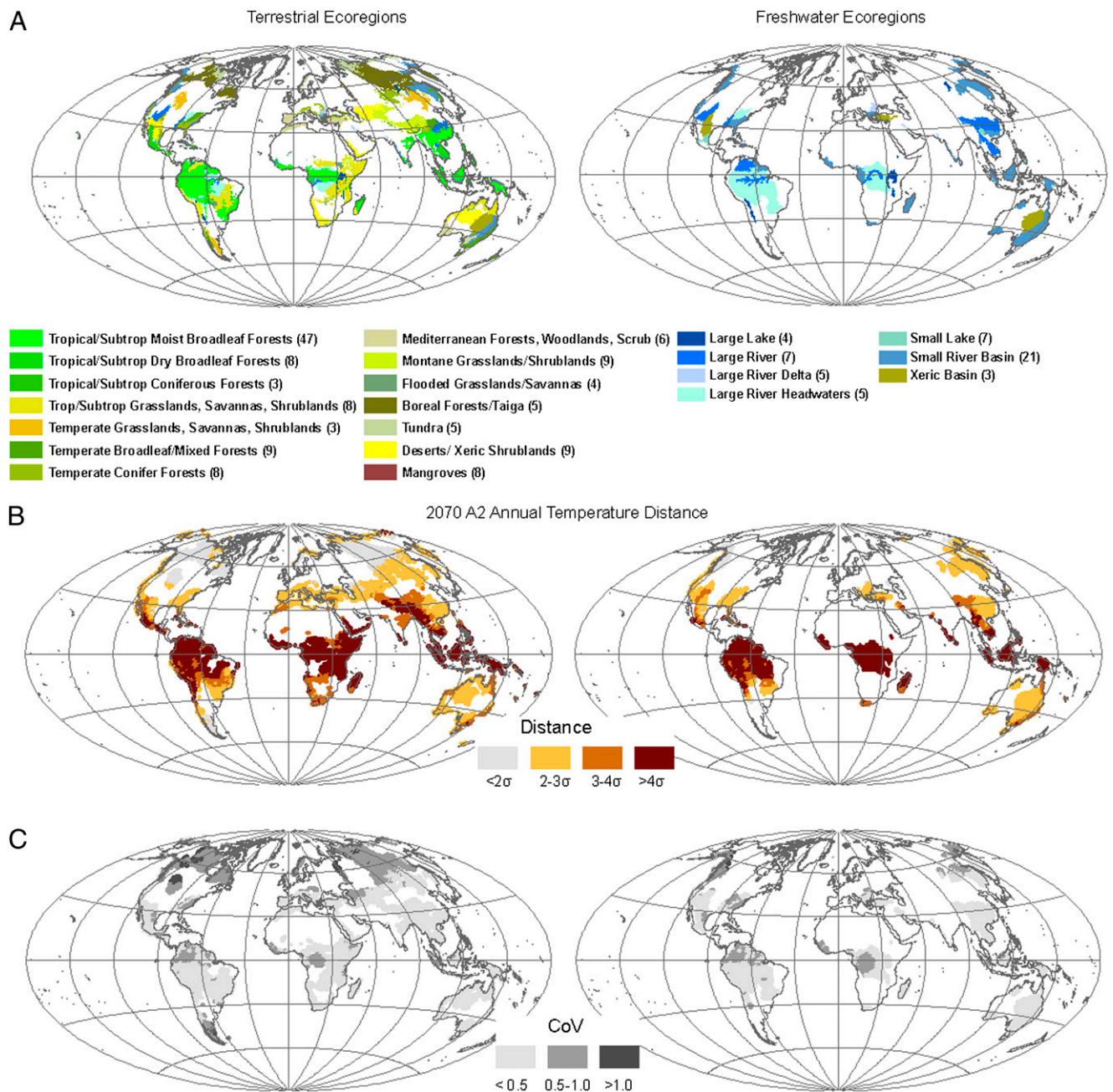


Fig. 1. Distribution of extreme monthly Tas_{μ} projected for 2070 across the terrestrial and freshwater components of WWF's Global 200. (A) The distribution of 132 terrestrial and 53 freshwater ecoregions, grouped by biomes. (B) Average distance of 21st century monthly Tas_{μ} from that of the baseline period (1961–1990), where distance is measured as SDs (σ) from the mean (μ) of the baseline. Extreme monthly Tas_{μ} is defined as exceeding 2σ of the baseline μ . Results are based on a climate model ensemble (n realizations = 173) for the A2 emission scenario. (C) The coefficient of variation (CoV) shows variation across different realizations within the climate model ensemble. Areas with higher values for CoV indicate greater differences across alternate projections of future Tas_{μ} and, hence, less certainty in distance values.

ensure that each climate model contributed equally to the final results. Thus, our ensembles provide comprehensive coverage of variability across projections of future climate.

Results

Across the climate model ensembles, average monthly temperature anomalies throughout the ecoregions are projected to range from 1.3 °C (± 0.4 °C) by 2030 to 2.6 °C (± 0.8 °C) by 2070 (Fig. S1). Shifts in monthly precipitation range from -11 to $+18\%$ by 2030 and -19 to $+26\%$ by 2070 (Fig. S2).

Although current rates of increase in CO₂ emissions are near the top of the SRES emission scenarios (19), making B1 projec-

tions unlikely, we present the range of results from the three emission scenarios. Within the next 20 y, the entire range of 12–22% (B1, A1B) of the world's most important terrestrial and freshwater ecoregions will face mean monthly temperature regimes beyond 2σ of the 20th century baseline period (Fig. S3). An additional 38–39% (B1, A1B) ecoregions will have at least a part of their range exceeding this threshold (Figs. S4 and S5). A local rise of <2 °C will mean that monthly Tas_{μ} across 66 terrestrial and 23 freshwater ecoregions will on average be extreme compared with the baseline period. This group includes some of the world's most biologically rich or unique regions, such as Chocó-Darién of South America, forest ecoregions of Sumatra and Peninsula

Malaysia, and the South African Fynbos. By 2070, the entire ranges of 60–86% (B1, A2) of 132 terrestrial and 51–83% (B1, A2) of 53 freshwater ecoregions will experience extreme monthly Tas_{μ} regimes (Tables S1 and S2). Most of the remainder will contain a mosaic of extreme and “typical” (i.e., within 2σ of the baseline period) monthly Tas_{μ} patterns. The exceptions under all three emission scenarios are two terrestrial (Ural Mountains Taiga/Tundra, Muskwa/Slave Lake Boreal Forests) and one freshwater ecoregion (Volga River Delta), which are projected to retain Tas_{μ} conditions typical to the baseline period across their entire range.

It has generally been expected that high-latitude regions will be more vulnerable to climate change than tropical areas, due to the faster rate of change being recorded in these regions and higher projected Tas anomalies (20), partly as a result of the ice albedo feedback (21). The AR4 (7, 13) reported a large number of physical and biological impacts already observed in high-latitude areas of the Northern Hemisphere (NH) compared with the tropics, although this trend may reflect a reporting bias. Extreme conditions are not absolute, but relative to the ecoregion of interest, based on the underlying temperature and precipitation distributions. A high σ in the high-latitude regions represents a larger climate amplitude, which reduces the likelihood of 2σ being systematically exceeded. In contrast, the low monthly Tas_{μ} variability of the tropics and subtropics (i.e., a smaller annual temperature range) infers that Tas_{μ} shifts because of warming will translate into extreme conditions with a smaller increase in temperature (Fig. 1B). Thus, monthly Tas_{μ} across some ecoregions in Africa is projected to exceed 2σ of the baseline period by 2030; by 2070, all terrestrial African ecoregions are projected to exceed 2σ . In contrast, this threshold is not exceeded across the entire range of any North American terrestrial ecoregion until 2050 or any European/north Asian (i.e. above 40N) terrestrial ecoregion until 2070 (Figs. S4 and S5). Further, local increases of 0.9–1.8 °C will result in areas within all African ecoregions experiencing extreme monthly Tas_{μ} .

Ecoregions in North America require Tas_{μ} increases of 0.7 to >5 °C (terrestrial) and 0.7–2.6 °C (freshwater) to impose extreme conditions (Tables S1 and S2).

Terrestrial ecoregions within the Tropical/Subtropical Moist Broadleaf Forests, Tropical/Subtropical Grasslands/Savannas/Shrublands, Flooded Grasslands/Savannas, and Mangrove biomes are projected to experience extreme monthly Tas_{μ} earliest. An increase in Tas_{μ} of <2.9 °C drives the entire range of all ecoregions within these biomes into extreme conditions, with the eight mangrove ecoregions projected to experience extreme conditions with <1.3 °C increase (Fig. 2). By 2070, ecoregions continuing to have areas with Tas_{μ} typical to the baseline occur primarily in the Boreal Forests/Taiga, Temperate Grasslands/Savannas/Shrublands and Forests, and Tundra biomes in the NH, although Tas_{μ} anomalies of up to 5.4 (Boreal Forests/Taiga) and 6.5 °C (Tundra) are projected (Fig. 2).

Of the 132 terrestrial ecoregions, 106 are classified as either vulnerable or CE (16). By 2070 under the A2 emission scenario, monthly Tas_{μ} is projected to exceed 2σ for all but one of these ecoregions (Ural Mountains Taiga and Tundra); 92 will face extremes > 3σ of the baseline period across at least part of their range. Although the remaining 26 terrestrial ecoregions are classified as “relatively stable” over the next 40 y, 9–14 will no longer contain any areas with monthly Tas_{μ} within 2σ of the baseline by 2050, depending on the emission scenario.

Across the freshwater ecoregions, those with the most extreme Tas_{μ} belong to river systems in Central Africa, such as the Congo River and Flooded Forests and Upper Guinea Rivers and Streams (Fig. 1B and Table S2). By 2070, the Volga River Basin will be the only freshwater ecoregion to contain Tas_{μ} < 2σ of the baseline across its entire range under all three emission scenarios: 8–26 other ecoregions will consist of mosaics of extreme and typical Tas_{μ} . Of the 31 freshwater ecoregions currently classified as CE,

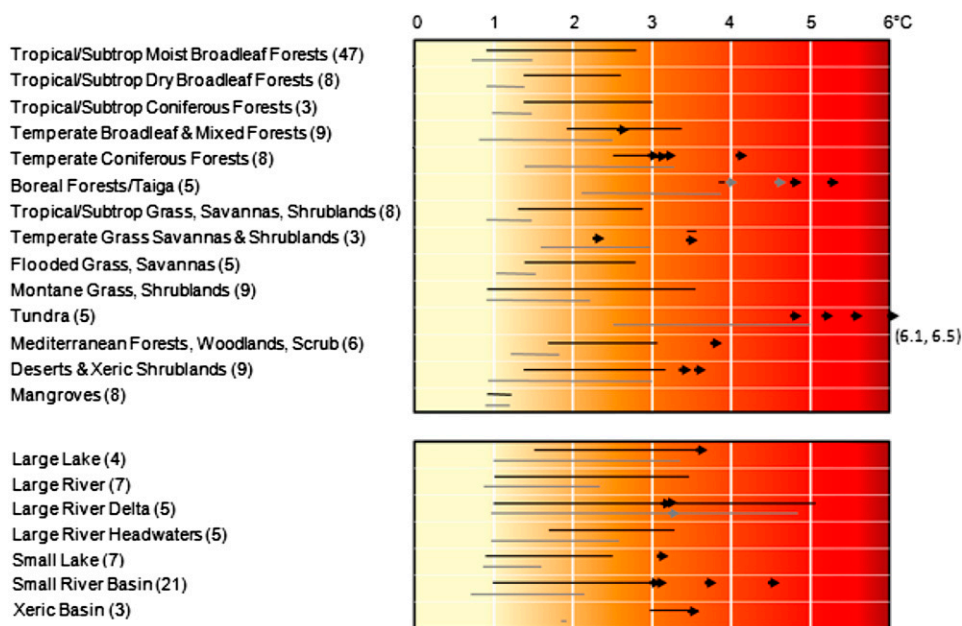


Fig. 2. Estimated local Tas anomaly required to produce extreme monthly Tas_{μ} across the Global 200 terrestrial and freshwater ecoregions. The number of ecoregions within each biome is given in parentheses. For a given biome, the black line shows the range of Tas anomalies required to drive the entire distribution of its ecoregions into extreme conditions. Some ecoregions do not have extremes of monthly Tas_{μ} projected to occur across their entire range by 2070. For these ecoregions, the black arrow indicates the average maximum Tas anomaly projected to occur within that ecoregion by 2070 (multiple black arrows for a given biome represent values for separate ecoregions). Thus, a Tas anomaly greater than this value is required for the entire range of these ecoregions to have extreme monthly Tas_{μ} . The gray line shows the range of Tas anomalies required for least one 1° grid cell of each ecoregion within the biome to have extreme monthly Tas_{μ} . Two ecoregions in the Boreal Forests/Taiga biome and one Large River Delta do not have any grid cells projected to be extreme. The maximum projected Tas anomaly for these regions is indicated by the gray arrows. Note: Values are a conservative estimate only, because they are based on average maximum Tas anomalies from the multimodel ensembles used for this study. It is possible that Tas anomalies smaller than these will result in extreme monthly Tas_{μ} conditions for the ecoregions. Results for individual ecoregions are in Tables S1 and S2.

nine are projected to be exposed to extreme conditions with Tas_{μ} increases $\leq 1.5^{\circ}\text{C}$.

In contrast to Tas_{μ} , monthly Pr_{μ} variability over the baseline period is high throughout all but low Pr_{μ} regions. Twenty-first century monthly Pr_{μ} does not exceed 2σ of the baseline period for any ecoregion under any of the emissions scenarios or time periods. Although there is no evidence for extreme precipitation magnitudes across the Global 200 until at least 2070, other changes in precipitation compared with the baseline climate (e.g., prolonged periods of surplus/deficit conditions, changes in the amount of total rainfall that occurs during events of given thresholds) will impact on the ecoregions.

For each ecoregion, we calculated the number of months where Tas_{μ} and Pr_{μ} are projected to exceed 2σ of the baseline period. Multimodel ensembles suggest that by 2050, the entire range of 6–26 (B1, A1B) terrestrial ecoregions from Tropical/Subtropical Moist Broadleaf Forests, Mangroves and Montane Grasslands/Shrublands, and two to seven (B1, A1B) freshwater ecoregions, from mainly smaller freshwater bodies, will face extreme monthly Tas_{μ} across all 12 mo. A further 91–103 terrestrial and 38–42 freshwater ecoregions will have at least 1 mo of extreme Tas_{μ} across their entire range. By 2070, this trend increases to 119–124 terrestrial and 51–52 freshwater ecoregions (Fig. 3). Even ecoregions with a conservation classification of Relatively Stable may face multiple months of extreme Tas_{μ} : As early as 2030, 13–15 (B1, A1B) such ecoregions have at least 6 mo a year where monthly Tas_{μ} exceeds 2σ of the baseline period across their entire range. In contrast to Tas_{μ} , projections of Pr_{μ} lie within 2σ of the baseline period for all 12 mo across the three emission scenarios.

The use of multiclimate model ensembles is a key attribute of this study. Climate models vary in their capacity to simulate the mean and variance of a specific variable within a specific region, and reliance on a small sample of models is therefore very likely to be misleading. Using a large ensemble minimizes biases associated with small samples of climate models and enables the identification of geographic areas where the results either agree or disagree within the ensemble. Across our ensembles variation in

projections of Tas_{μ} is low for most of Africa and South America, increasing confidence in these results. Greater variability among realizations occurs within higher latitude regions, suggesting lower confidence in the simulations of future Tas_{μ} regimes across these areas (Fig. 1C).

Although climate models unanimously project global temperature increases throughout the course of this century, substantial variability occurs in projections of precipitation changes (22). Thus, although weighted monthly Pr_{μ} does not exceed 2σ of the baseline period in any ecoregions, averaging across the components of climate model ensembles obscures variability. For example, for 8–13 ecoregions (2030, 2070), at least 25% of realizations projected that the threshold of 2σ will be exceeded. In the case of eight ecoregions (Indochina Dry Forests, Eastern Himalayan Broadleaf and Conifer Forests, Altai-Sayan Montane Forests, Sudanian Savannas, Daurian/Mongolian Steppe, Tibetan Plateau Steppe, Mekong River, Salween River), >50% of realizations for 2070 (A1B, A2) projected this threshold to be exceeded across 1–9 mo. This trend indicates that there is a greater likelihood of these regions experiencing extreme Pr_{μ} regimes than the mean weighted value suggests. The proportion of realizations projecting the threshold to be exceeded is greatest primarily in June, July, and August.

Variation in the extent to which temperature and precipitation are correlated may exacerbate or lessen the impacts of climate change. By 2070, the correlation coefficient (r) for 18–33% (B1, A2) of terrestrial and freshwater ecoregions is projected to strengthen or weaken, or change sign, by at least 0.1 for one or more seasons. In the majority of cases, this trend represents a strengthening of a currently negative correlation or weakening of a positive correlation, i.e., r decreases (37%, 32% of cases respectively) (Table S3). Changes in r are considerable for some ecoregions: The correlation between temperature and precipitation across the Amazon River and Flooded Forests is projected to change by >0.2 across each season [e.g., March–April–May: baseline $r = -0.04$; 2070 (A2) $r = -0.4$]. Similarly, throughout the Guianan Moist Forest, the negative correlation strengthens by >0.2 over December–January–February and September–

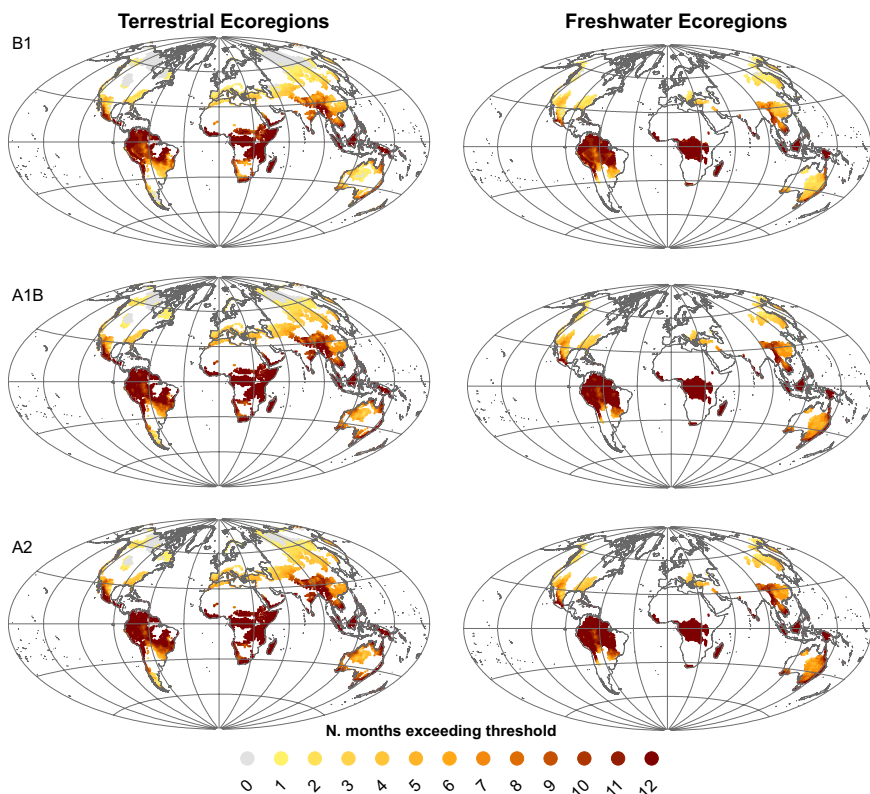


Fig. 3. The number of months by 2070 where monthly Tas_{μ} is projected to exceed thresholds of 2σ across terrestrial or freshwater ecoregions, under three emission scenarios (B1, A1B, and A2).

October–November. In contrast, all ecoregions within the Tropical and Subtropical Coniferous Forests, Grasslands/Savannas/Shrublands, and Large Lake biomes are projected to undergo only minor changes in correlation (i.e., <0.1) (Mangroves were not included in analyses because of the small number of grid cells covered by these ecoregions).

Discussion

Our results suggest that climate change projected to occur over the coming decades may place substantial strain on the integrity and survival of some of the most biologically important ecoregions worldwide. Within the next 60 y, almost all of the Global 200 ecoregions will face monthly Tas_{μ} conditions that could be considered extreme based on the 1961–1990 baseline period. Many of these regions are already exposed to substantial threats from other environmental and social pressures (16): These, combined with climate impacts, increase the likelihood of their loss over the 21st century. Standard conservation practices may prove insufficient for the continuation of many of these ecoregions (23).

Our analysis suggests that tropical and subtropical ecoregions in Africa and South America may be particularly vulnerable to climate change. Not only will developing countries in these regions be less capable to mitigate climate impacts, but Tas_{μ} will become extreme with relatively small increases in local temperatures. We do not suggest that the absolute temperatures in the tropics will rise more than in the higher latitudes. Rather, the increase in absolute temperatures relative to the past variability will be larger in the tropics than in higher latitudes. Thus, the climate forcing on ecoregions in the tropics will become extreme with a smaller increase in temperature. In addition, increases in temperature may result in higher vapor pressure deficits (VPD) and evaporation, thereby reducing the availability of water for plant growth. Higher mean annual temperatures in the Southern Hemisphere (SH) compared with the NH and the nonlinear relationship between temperature, autotrophic respiration, and vapor pressure suggest that increases in temperature in the SH will reduce water availability to a greater extent than the same increases in temperature in the NH (14). Although net primary productivity (NPP) in tropical ecosystems increased over the last two decades of the 20th century (24), large-scale temperature-induced drying reduced NPP in South America during the first decade of this century (14). Projected decreases in precipitation over the Amazonian dry season (June/July to October/November) and a strengthening of the negative correlation between Tas_{μ} and Pr_{μ} from June to August may exaggerate the impacts of higher temperatures.

Whether and when extreme climate conditions will result in substantial species turnover and dramatic changes within the ecosystems of the Global 200 will depend, in part, on their exposure to other human-induced pressures, their inherent capacity to adapt to new conditions, the presence of thresholds/tipping points and time lags in responses. For example, deforestation of mangroves is occurring at a rate of 1–2% per year: Losses between 35% and 86% have already occurred, with rates increasing rapidly in developing countries (25). Based on sea level rises only, it has been estimated that mangroves may decline by 10–15% by 2100, with those occupying low-relief islands being particularly vulnerable (26). Thus, over the course of this century, deforestation may result in much greater loss of mangroves than climate change. However, our results show that mangroves require only a small rise in local temperatures (<1.3 °C) for monthly Tas_{μ} to become extreme. Exposure to heat-stress resulting from extreme monthly temperatures will place additional pressure on the resilience of mangroves.

Biota within many of the Global 200 ecoregions will be limited in their ability to respond with range shifts, such as those at high altitude (e.g., Central Range Subalpine Grasslands, Indonesia/Papua New Guinea), on small islands (e.g., New Caledonian Moist and Dry Forests and Streams, South Pacific Islands Forests), or those that require large geographic displacements to track changing climates (particularly ecoregions in flooded grassland, mangrove and desert biomes; ref. 27). Further, current land-use practices and high levels of human footprint (28) in surrounding

regions and/or proximity to geographic barriers make it unlikely that many ecoregions projected to face extreme conditions soonest will be able to migrate to new areas (e.g., Everglades Flooded Grasslands, USA; Southwestern Ghats Moist Forest, India). Compared with biomes in other locations, vast areas extending across Russia, western China, and Mongolia have been exposed to relatively few human impacts (28) such as habitat fragmentation. It is more feasible that ecoregions in these locations will be able to track climate change compared with ecoregions surrounded by highly fragmented and disturbed landscapes.

Our study suggests that it is Boreal/Taiga and Tundra ecoregions at high latitudes in the NH that will be less likely to experience extreme Tas_{μ} until (at least) 2070. However, biotic responses coinciding with 20th century warming have already occurred, including recent forest expansion in the Urals (29), increased biomass in Arctic plant communities (30), collapses in population cycles of herbivores (31), and changes to NPP (14). Productivity of ecoregions in cold climates is primarily limited by low temperature. Shifts in Tas_{μ} will release climatic constraints imposed on these regions. However, lower net CO_2 uptake in high-latitude ecosystems has occurred during hotter and drier summers (32). This trend suggests that, although some high-latitude ecoregions are projected to experience monthly Tas_{μ} within the range of the baseline period until at least 2070, strengthening of a negative correlation between Tas_{μ} and Pr_{μ} (such as that projected to occur across the Fenno-Scandian Alpine Tundra and Taiga ecoregion) may limit the growing season CO_2 uptake.

In addition to shifts in mean climatic conditions, climate variability has recently been demonstrated to impact the spatial distribution of species (33), and increasing climatic variability (34) may impose a growing influence on species and ecosystems. We have used monthly timescales to assess the vulnerability of the Global 200 and have not incorporated changes in variability. Our results may therefore underestimate the impact of climate change on these biota as the emergence of rare temperatures not presently experienced, and not visible in a monthly mean, is likely to have immediate impacts. We encourage experts in the behavior of specific ecoregions to explore how exposure to extremes, and changes in correlations, may exacerbate the vulnerability of these ecoregions to future climate change.

Methods

Creation of Climate Model Ensembles. We created three sets of ≈ 200 -member ensembles of simulations from multiple fully coupled climate models for the A1B, A2, and B1 emissions scenarios for 2030, 2050, and 2070. These three emissions scenarios were chosen as they represent a range of CO_2 concentrations by the end of the 21st century, and because at least 15 of the 23 AR4 climate models resolved monthly data for one or more of the scenarios. Future climate data were obtained from the Program for Climate Model Diagnosis and Intercomparison (www.pcmdi.llnl.gov), which hosts climate model (GCM) data used in the Intergovernmental Panel on Climate Change Fourth Assessment Report (AR4). Data were available for 23 climate models, although different models report for different climate variables, emissions scenarios and with different numbers of realizations (alternate runs of a GCM). We downloaded monthly data from all GCMs that simulated both monthly precipitation (Pr) and average near surface air temperature (Tas). Fifteen GCMs provide data for more than one realization of either 20th century or 21st century climate, and these realizations were combined to provide a larger number of datasets. For example, CCCMA models report five realizations for the 20th century climate and five for each of the three emissions scenarios. These were combined into 25 different realizations for each emission scenario. Extending this over all available models gives 214 (B1), 223 (A1B), and 173 (A2) realizations (Table S4).

Climate impact studies typically calculate the change in a climate variable as the difference between a value at some point in the future, usually averaged over a 30-y period, compared with a similar length period in the 20th century. For each realization, we extracted 30-y average monthly data for four time periods: 1961–1990 (baseline climate), 2016–2045, 2036–2065, and 2056–2085, for Tas and Pr . Tas anomalies were calculated by subtracting future temperature from the baseline temperature, whereas differences for Pr were expressed as ratios (future/baseline). The baseline climate was extracted from the Climate of the 20th Century scenario (20c3m simulation) individually for each model and realization. As the GCMs have different resolutions, spanning $\approx 1.5^\circ$ to 5° , we interpolated all models to a common grid resolution of

1° latitude/longitude by using a nearest neighbor method (command RESAMPLE in ArcGIS v9.2). Although interpolation of the models to a common grid allows for calculations to be performed across all models, it does not improve the quality of the model's simulation. Errors that occur in a given GCM, due to any number of reasons (e.g., convective precipitation parameterization, ice, and albedo feedbacks, and lack of a carbon cycle), will affect projections whether the model is used at its native or interpolated resolution.

Monthly time-series datasets for the baseline period of 1961–1990 were obtained from the Climatic Research Unit, University of East Anglia (www.cru.uea.ac.uk/cru/data/hrg.htm), at a resolution of 0.5°, averaged over 1°, and incorporated with climate anomalies to produce future climate scenarios.

Global 200 Ecoregions. Digital data on the Global 200 Ecoregions was obtained from the World Wildlife Fund (www.worldwildlife.org/science/ecoregions/global200.html). The terrestrial and freshwater ecoregion (and associated biome) at the center-point of each 1° grid cell was extracted. Digital data for the G200 includes 142 terrestrial ecoregions; however, 11 were too small for inclusion in our study (see regions 11, 19, 32, 38, 50, 53, 60, 104, 107, 126, 132; ref. 16), and one (region 147, Amazon River and Flooded Forests) was included in the original dataset as both a terrestrial and freshwater ecoregion (spanning slightly different extents). Therefore, our study is limited to 132 terrestrial and 53 freshwater ecoregions (Tables S1 and S2).

Analyses. We assess the extent to which the Global 200 ecoregions are projected to be exposed to average monthly Tas_{μ} and Pr_{μ} patterns during the 21st century, which could be considered extreme compared with the 20th century baseline (1961–1990). We calculated the standardized Manhattan Distance (M) for both monthly Tas_{μ} and Pr_{μ} as the distance between the mean (μ) 21st century value and the mean of the 1961–1990 baseline, standardized by the SD (σ) of the baseline climate (23). These values are location-dependent, that is, they were calculated for each 1° grid cell such that

$$M = ((21^{th}C \mu - 20^{th}C \mu) / \sigma(20^{th}C)).$$

Where the σ of Pr over the baseline climate equaled 0, M was set to the value of the anomaly.

A value of 2σ represents a good approximation for identifying extreme climate (35). Thus, following ref. 17, we defined extreme monthly Tas_{μ} and

Pr_{μ} as exceeding 2σ of the baseline μ (i.e., $M > 2$). For each of the three 21st century time periods, we calculated the average monthly M and the number of months where Tas_{μ} and Pr_{μ} were projected to exceed the extreme of 2σ . Most ecoregions span more than one 1° grid cell. Therefore, we assessed whether (i) all grid cells or (ii) at least one 1° grid cell within a given ecoregion exceeded the extreme of 2σ .

We recognize that our methods make several approximations that may not always be adequate: (i) climate of the baseline period is normally distributed (a reasonable assumption for temperature, however precipitation is frequently skewed (e.g., ref. 36) and, thus, its sensitivity may be underestimated) and (ii) climate variability remains stationary into the future. This second assumption is likely to be wrong as evidence exists for changes in persistence of drought, and in the frequency and intensity of rainfall (37). Greater climate variability would be expected to have higher impacts on biota compared with our estimates.

The climate model ensembles created for each emission scenario incorporated different numbers of realizations (ranging from 1 to 72) from the various climate models. We calculated the weighted mean M from all realizations of the ensemble. Weights of each realization were normalized so they summed to 1, with each climate model contributing an equal weight. Therefore, the weighted mean M of the ensemble is:

$$\sum_{i=1}^n w_i = 1,$$

where w_i is the weight of realization i from climate model j .

The coefficient of variation, based on the weighted mean and weighted SD was also calculated to show variability across the different realizations comprising each ensemble. Furthermore, for each ecoregion spanning at least $10 \times 1^\circ$ grid cells ($n = 134$), we calculated Pearson's Correlation Coefficient for seasonal (December–February, March–May, June–August, September–November) temperature and precipitation by using Cran-R (38).

ACKNOWLEDGMENTS. We thank L. Hughes, P. Wilson, and J. VanDerWal for reading the manuscript. L.J.B. was supported by an Australian Research Council (ARC) Post-doctoral Fellowship, and L.J.B. and A.J.P. were supported by ARC Discovery Project DP087979. W.T., N.E.Z., and N.G.Y. were funded by Sixth European Framework Programme Ecochange Project Grant GOCE-CT-2007-036866.

- Butchart SHM, et al. (2010) Global biodiversity: Indicators of recent declines. *Science* 330:329–330.
- Rands MRW, et al. (2010) Biodiversity conservation: Challenges beyond 2010. *Science* 330:329–330.
- Pereira HM, et al. (2010) Scenarios for global biodiversity in the 21st century. *Science*, 330:1496–1501. [10.1126/science.1196624](https://doi.org/10.1126/science.1196624).
- Thomas CD, et al. (2004) Extinction risk from climate change. *Nature* 427:145–148.
- Stork NE (2010) Re-assessing current extinction rates. *Biodivers Conserv* 19:357–371.
- Brook BW, Sodhi NS, Bradshaw CJA (2008) Synergies among extinction drivers under global change. *Trends Ecol Evol* 23:453–460.
- IPCC (2007) *Climate Change 2007: The Physical Basis. Contribution of Working Group I to the Fourth Assessment Report of the Intergovernmental Panel on Climate Change* (Cambridge Univ Press, Cambridge, UK).
- Walther G-R, et al. (2009) Alien species in a warmer world: Risks and opportunities. *Trends Ecol Evol* 24:686–693.
- Root TL, MacMynowski DP, Mastrandrea MD, Schneider SH (2005) Human-modified temperatures induce species changes: Joint attribution. *Proc Natl Acad Sci USA* 102:7465–7469.
- Root TL, et al. (2003) Fingerprints of global warming on wild animals and plants. *Nature* 421:57–60.
- Cleland EE, Chuine I, Menzel A, Mooney HA, Schwartz MD (2007) Shifting plant phenology in response to global change. *Trends Ecol Evol* 22:357–365.
- Parmesan C (2006) Ecological and evolutionary responses to recent climate change. *Annu Rev Ecol Syst* 37:637–669.
- IPCC (2007) *Climate Change 2007: Impacts, Adaptation and Vulnerability. Contribution of Working Group II to the Fourth Assessment Report of the Intergovernmental Panel on Climate Change* (Cambridge Univ Press, Cambridge, UK).
- Zhao M, Running SW (2010) Drought-induced reduction in global terrestrial net primary production from 2000 through 2009. *Science* 329:940–943.
- Thuiller W (2007) Biodiversity: climate change and the ecologist. *Nature* 448:550–552.
- Olson DM, Dinerstein E (2002) The Global 200: Priority Ecoregions for Global Conservation. *Ann Mo Bot Gard* 89:199–224.
- Palmer TN, Räisänen J (2002) Quantifying the risk of extreme seasonal precipitation events in a changing climate. *Nature* 415:512–514.
- Piao S, Friedlingstein P, Ciais P, Zhou L, Chen A (2006) Effect of climate and CO₂ changes on the greening of the Northern Hemisphere over the past two decades. *Geophys Res Lett*, 33: 10.1029/2006GL028205.
- Manning MR, et al. (2010) Misrepresentation of the IPCC CO₂ emission scenarios. *Nat Geosci* 3:276–277.
- Christensen J, et al. (2007) Regional Climate Projections. *Climate Change 2007: The Scientific Basis Contribution of Working Group I to the Fourth Assessment Report of the Intergovernmental Panel on Climate Change*, ed Solomon S (Cambridge Univ Press, Cambridge, UK).
- Dickinson R, Meehl G, Washington W (1987) Ice Albedo feedback in a CO₂ doubling simulation. *Clim Change* 10:241–248.
- Solomon S, et al. (2007) 2007: Technical Summary. *Climate Change 2007: The Physical Science Basis Contribution of Working Group I to the Fourth Assessment Report of the Intergovernmental Panel on Climate Change*, eds Solomon S, et al. (Cambridge Univ Press, Cambridge, UK).
- Williams JW, Jackson ST, Kutzbach JE (2007) Projected distributions of novel and disappearing climates by 2100 AD. *Proc Natl Acad Sci USA* 104:5738–5742.
- Nemani RR, et al. (2003) Climate-driven increases in global terrestrial net primary production from 1982 to 1999. *Science* 300:1560–1563.
- Duke NC, et al. (2007) A world without mangroves? *Science* 317:41–42.
- Alongi DM (2008) Mangrove forests: resilience, protection from tsunamis, and responses to global climate change. *Estuar Coast Shelf Sci* 76:1–13.
- Loarie SR, et al. (2009) The velocity of climate change. *Nature* 462:1052–1055.
- Sanderson EW, et al. (2002) The human footprint and the last of the wild. *Bioscience* 52:891–904.
- Devi N, et al. (2008) Expanding forests and changing growth forms of Siberian larch at the Polar Urals treeline during the 20th century. *Glob Change Biol* 14:1581–1591.
- Hudson JMG, Henry GHR (2009) Increased plant biomass in a High Arctic heath community from 1981 to 2008. *Ecology* 90:2657–2663.
- Ims RA, Henden J-A, Killengreen ST (2008) Collapsing population cycles. *Trends Ecol Evol* 23:79–86.
- Angert A, et al. (2005) Drier summers cancel out the CO₂ uptake enhancement by warmer springs. *Proc Natl Acad Sci USA* 102:10823–10827.
- Zimmermann NE, et al. (2009) Climatic extremes improve predictions of spatial patterns of tree species. *Proc Natl Acad Sci USA* 106(Suppl 2):19723–19728.
- Schär C, et al. (2004) The role of increasing temperature variability in European summer heatwaves. *Nature* 427:332–336.
- Luterbacher J, Dietrich D, Xoplaki E, Grosjean M, Wanner H (2004) European seasonal and annual temperature variability, trends and extremes since 1500. *Science* 303:1499–1503.
- Perkins S, Pitman A, Holbrook N, McAvaney J (2007) Evaluation of the AR4 climate models' simulated daily maximum temperature, minimum temperature and precipitation over Australia using probability density functions. *J Clim* 20:4356–4376.
- Sun Y, Solomon S, Dai A, Portmann RW (2007) How often will it rain? *J Clim* 20:4801–4818.
- R Core Development Team (2010) R: A Language and Environment for Statistical Computing. (R Foundation for Statistical Computing, Vienna), Version 2.11.0.